Differentiating Supersymmetric Decay Chains Using Full-Simulation Data

Candidate Number: 8142R
Supervisor: Dr Christopher Lester

May 15, 2006

Abstract

The possibility of distinguishing events with different squark flavours in a SUSY cascade decay chain at ATLAS was considered, using a full-simulation of the detector. A system was devised for separating events with decay chains containing the first and second generation squarks from those with the third generation by using a cut on the number of b-jets. This gave a good efficiency but poor rejection. An attempt was made to distinguish the events with decay chains containing the sbottom from those containing the stop using a missing energy cut, but this gave poor efficiency and poor rejection. A method for distinguishing these two types of event by reconstructing W bosons and top quarks (known to be in stop events from the Monte Carlo truth record) was tried. However, this reconstruction proved impossible. A brief investigation was made into why this should be impossible, and some correlations were found between the Monte Carlo truth record of the W boson four-momentum and the missing transverse momentum. Further work is needed to establish a better method for distinguishing SUSY decay chains and investigating the precise reasons we failed to reconstruct the W bosons in stop events.

1 Introduction

1.1 The Standard Model and Beyond

The Standard Model (SM) provides a remarkably accurate description of high energy physics observed to date. However, the standard model is incomplete and requires new physics at higher energy scales. This will certainly be true at the reduced Planck scale $\overline{M}_{PL} = (8\pi G)^{-1/2} = 2.4 \times 10^{18}$ GeV, where quantum gravitational effects become important.

One challenge posed to the SM is the so-called "hierarchy problem" – without some new physics, the Higgs scalar boson mass, m_H, becomes very large, $\mathrm{O}(\overline{M}_{PL})$. This is because the Higgs couples to fermions, so every fermion loop diagram (for example, Figure 1(a)) contributes to m_H. Any momentum can circulate in the fermion loop in Figure 1(a), making m_H potentially infinite. However, we already expect new physics beyond the SM so we cut-off the integral at some energy, Λ_{UV}. If we choose Λ_{UV} to be the Planck mass, we get a Higgs mass which is $\mathrm{O}(\overline{M}_{PL})$, because the fermion loops contribute divergent terms in Λ_{UV}. However, we expect a Higgs mass which is roughly O(100 GeV).

To fix the hierarchy problem in a natural way, Supersymmetry (SUSY) has been proposed. This postulates a hitherto unobserved symmetry of nature relating fermions and bosons. In SUSY, each quark and lepton in the SM has two scalar *superpartners* with matching couplings. These will give corrections to m_H of the form shown in Figure 1(b), completely cancelling

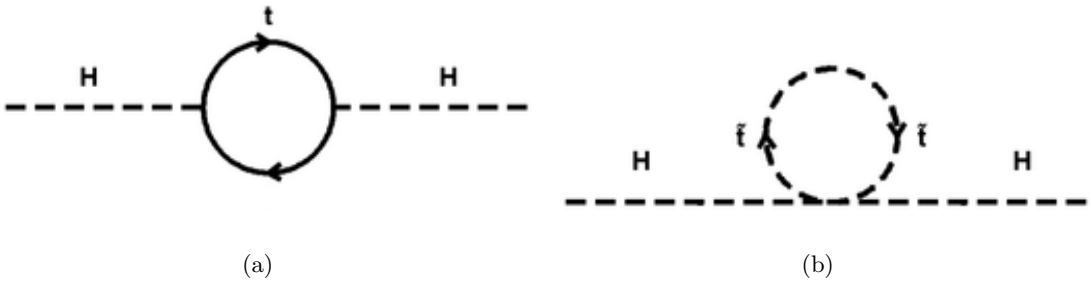

(a) (b)

Figure 1: Example Feynman diagrams showing (a) a fermionic (top quark) loop correction to the Higgs mass (b) a scalar (stop squark) correction to the Higgs mass.

the divergent terms. By assuming SUSY, the hierarchy problem is neatly solved; this is the primary motivation for such theories.

Each fermion in the SM has a left- and right-handed chiral component, expressed as separate Weyl spinors. SUSY adds a scalar partner to each Weyl spinor, giving the required two scalars per fermion. Each scalar can be labelled as 'left' or 'right' according to which Weyl spinor is its superpartner. Note that these scalars are not themselves chiral. They are named by prefixing and 's' to the name of their SM partner, and labelled with a tilde, e.g. the left-handed component of the up quark u_L has the left sup squark $\tilde{u}_L$ as its superpartner. SUSY also postulates fermionic (spin 1/2) superpartners for the gauge vector bosons of the SM and the Higgs sector. These are referred to as winos ($\tilde{W}^{\pm}, \tilde{W}^0$), binos ($\tilde{B}^0$), gluinos ($\tilde{g}$) and higgsinos ($\tilde{H}_u^+, \tilde{H}_u^0, \tilde{H}_d^0, \tilde{H}_d^-$) respectively. Winos, binos and higgsinos mix to form four neutral gauginos (neutralinos, $\tilde{\chi}_{1-4}^0$) and four charged gauginos (charginos, $\tilde{\chi}_{1-2}^{\pm}$). Furthermore, significant mixing is expected between the two stops, sbottoms and staus and the resulting physical mass eigenstates are labelled with a subscript 1 or 2. This set of states is the minimum required for SUSY and makes up the Minimal Supersymmetric Standard Model (MSSM).

The MSSM as it stands allows violation of baryon number, B, and lepton number, L, at rates much higher than experimentally allowed. Hence, the MSSM introduces a further symmetry to eliminate this. This new symmetry is a multiplicatively conserved quantum number called "R-parity", $R_P = (-1)^{3(B-L)+2s}$, where s is spin. All SM particles have $R_P = +1$ and all SUSY particles have $R_P = -1$. R_P conservation has two important consequences:

- SUSY particles must be produced in pairs in collider experiments.
- The Lightest SUSY Particle (LSP) is absolutely stable and each sparticle must decay to it. If it is neutral and weakly interacting, it will escape detection at collider experiments and provide missing energy.

If SUSY were an *exact* symmetry, the SUSY particles would have the same masses as their SM partners. This is experimentally ruled out, so SUSY must be broken in the current vacuum ground state. SUSY is said to be broken by an unknown "hidden sector", because the MSSM alone cannot account for this symmetry breaking. "Soft" SUSY breaking introduces new terms in the SUSY Lagrangian involving only the SUSY particles, explicitly breaking the symmetry. It also introduces 105 new parameters, but this is vastly reduced if the interactions are flavour blind. Gravity is an excellent candidate for such an interaction. Supergravity (SUGRA) theories postulate that the hidden sector communicates with the MSSM via gravitational-type interactions. Minimal Supergravity (mSUGRA) models have only five

parameters, $m_{1/2}, m_0, A_0, \tan\beta$ and $\text{sgn}(\mu)$. The first three are the fermionic mass parameter, the scalar mass parameter and the trilinear scalar coupling; $\tan\beta$ and $\text{sgn}(\mu)$ relate to the Higgs-higgsino sector. mSUGRA also introduces a gravitino with mass $m_{3/2}$. A full discussion of mSUGRA is far beyond the scope of this Introduction. For reference, the particular mSUGRA model considered in the present work uses $m_0 = 100$ GeV, $m_{1/2} = 300$ GeV, $A_0 = -300$ GeV, $\tan\beta = 6$, and $\text{sgn}(\mu) = +$. For a thorough discussion of SUSY and SUSY breaking, see [10] and references therein.

1.2 The Large Hadron Collider and the ATLAS Detector

The Large Hadron Collider (LHC) is a machine for colliding protons head-on with a centre of mass energy of 14 TeV, in a circular tunnel 27 km in circumference. A Toroidal LHC ApparatuS (ATLAS) is a general-purpose detector for the LHC experiment. It has four major components, the inner tracker which measures the momentum of charged particles, the calorimeter which measures particle energies, the muon detector and tracker and the magnet system, for bending charged particles for momentum measurements[9]. It has excellent capabilities for measuring the products (hadronic jets, electrons, muons, photons) of proton-proton collisions and measuring missing energy (see later).

ATLAS uses a right-handed coordinate system; ϕ is the azimuthal angle measured clockwise from the positive $x-$axis (which points into the LHC ring), looking into the positive $z-$direction (along the beam line). The polar angle θ is measured from the the positive z-axis. Pseudo-rapidity, $\eta = -\log(\tan\frac{\theta}{2})$ is used in preference to θ, because it is invariant under longitudinal Lorentz boosts. Hence, the quantity $\Delta R^2 = \Delta\eta^2 + \Delta\phi^2$ is also invariant and ΔR is used to measure how close two four-vectors are in this coordinate system ($\Delta\eta$ and $\Delta\phi$ are the differences in their η and ϕ coordinates respectively).

If supersymmetric particles exist and have masses of less than about 1 TeV, then it is expected that the LHC will operate at a high enough energy to produce them by proton-proton collisions, and ATLAS will be able to detect the decay products.

1.3 B-Jet Tagging and Missing Energy

ATLAS is capable of detecting b-jets (that is, jets that contain a b quark) and measuring the missing energy in an event. These will be important for our later physics analysis.

B-jet tagging is possible because b-hadrons have a relatively long lifetime (~ 1.5 ps) and will decay at a secondary vertex at a measurable distance (~ 4 mm for a 50 GeV particle) from the primary vertex (interaction point). By detecting such secondary vertices and measuring the impart parameters of jets produced from them relative to the primary vertex, a b-tagging weight can be assigned to a jet, assessing how likely it was such a jet contained a b-hadron. The best b-tagging performance at ATLAS is currently a combination of these two methods, and this is the weight we used. If the weight assigned is above some cut value, we considered a tagged jet to be a b-jet. A good cut to choose based on current data for b-jet tagging is requiring a b-tagging weight greater than 3. This means a high proportion of true b-jets are accepted and few light jets are falsely accepted[8].

Missing energy refers to energy which is not detected but which is expected from conservation laws. In hadron colliders, the total initial momentum is not known because it is divided between the hadron's constituents. This means it is impossible to calculate the total missing energy. However, the initial momentum transverse to the beam direction is known to be zero, so any net transverse momentum indicates missing energy. Hence, ATLAS is capable of measuring the missing transverse momentum of an event[2].

1.4 Full Simulation of the ATLAS Detector

In this project we hope to assess the distinguishability of different flavour decay chains containing SUSY particles at ATLAS, using full-simulation data. Though ATLAS will not begin collecting results until 2007, simulated data already exists. Full-simulation involves carrying out a full chain of steps in software to produce a detailed simulation of the detector[9]. So-called fast simulation (ATLFAST)[11][2] has been used for quick, approximate estimates of signals and backgrounds at ATLAS. Full-simulation is CPU intensive and slow compared to fast simulation, so most studies to-date have been done using ATLFAST. Full simulation can be used to check detector performance in detail (see [5], for example). The final step in the full chain is production of Analysis Object Data (AOD) files. Because of the difficulty in producing full-simulation AOD files, the files we used were centrally produced[1][1].

AOD files contain the simulated *reconstructed detector output* (which we will refer to as reconstructed data for short). Raw data from the detector comes as "hits" (signals produced by particles interacting with the various layers of the detector) which have to be "reconstructed"[2] to give information which is meaningful for physics analysis. AODs also contain the Monte Carlo truth record of the event[7] (which we will refer to as the truth information, or simply the truth), given by the software that generated the data. This is useful for seeing what "really" happened compared to what the reconstructed data says. One must be careful when using the truth record though, as it was not designed with this purpose in mind. A single particle will sometimes appear multiple times and this must be taken into account when considering the truth information.

AOD files are organised into different "containers" of all the data. For example, there is a container of reconstructed hadronic jets and a separate container of b-tagged jets. We used the Athena software framework[9] to access the data in the containers (see also Appendix A:).

1.5 A SUSY Decay Chain

In this project, we are interested in identifying the flavour of the parent squark in the decay chain shown in Figure 2. This is a 'cascade' chain, where each state decays to a lighter state. In SUSY, the masses of the $\tilde{d}$, $\tilde{u}$, $\tilde{s}$ and $\tilde{c}$ squarks are expected to be nearly degenerate and $\tilde{b}$ and $\tilde{t}$ are expected to have different masses to each other and to $\tilde{d}$, $\tilde{u}$, $\tilde{s}$ and $\tilde{c}$ (though the precise nature of the SUSY mass spectrum is unknown). The first and second generation squarks $\tilde{d}$, $\tilde{u}$, $\tilde{s}$ and $\tilde{c}$ are expected to decay in roughly the same way but $\tilde{b}$ and $\tilde{t}$ to decay differently. It is this insight that motivates the present analysis. It would be useful to perform this separation for future SUSY analyses and investigating the SUSY mass spectrum.

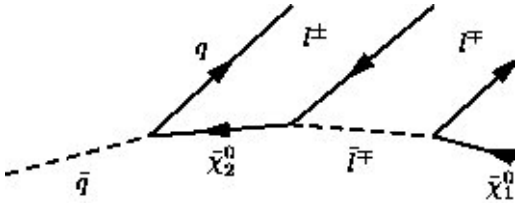

Figure 2: Feynman diagram of the decay chain we are considering in this project. $\tilde{q}$ can be any squark but $\tilde{l}$ must be $\tilde{e}$ or $\tilde{\mu}$. The flavour of q and l are physically constrained by $\tilde{q}$ and $\tilde{l}$ respectively.

[1]Little up-to-date information about using full-simulation and computing at ATLAS has been written up formally. Usually one must refer to web pages and talk slides.

We are interested only in a small subset of the possible squark decay chains. We define four "categories" of event: events which contain the decay chain in Figure 2 with a $\tilde{d}$, $\tilde{u}$, $\tilde{s}$ or $\tilde{c}$ squark exactly once, events which contain the chain with a $\tilde{b}$ squark exactly once, events which contain the chain with a $\tilde{t}$ squark exactly once and events with zero, two or more copies of the chain in any flavour[2]. The primary aim is to distinguish between these four categories of event using data from a full-simulation of the ATLAS detector.

We do not consider events which contain a $\tilde{\tau}$ in the decay chain (see Figure 2), because these decay to τ leptons which in turn will decay by a variety of messy processes[6]. This would only add confusion to the signal. Note that the end point of the chain is $\tilde{\chi}_1^0$, the LSP. This is expected to escape without the detection resulting in missing energy in each event. The two Opposite Sign Same Flavour (OSSF) leptons leaving the chain are a very distinct signature for its presence. The branching ratio to this chain for all flavours is only $\sim 5\%$, so we analyse $\sim 80,000$ events to gather appreciable statistics.

1.6 Distinguishing Events with the Chain Once

A series of cuts for separating events which contain our decay chain exactly once from other events has already been proposed[3]. Specifically, each event must satisfy the following conditions:

- Exactly two leptons, both OSSF and both with transverse momentum, $p_T > 10$ GeV.
- Four or more jets, all with $p_T > 50$ GeV and the highest p_T jet with $p_T > 100$ GeV.
- Missing transverse momentum $\not{p}_T \geq \max(100 \text{ GeV}, 0.2M_{effective})$ and $M_{effective} \geq 400$ GeV where $M_{effective}$ is defined by the scalar sum of the missing transverse energy and the p_T of the four highest p_T jets.

Because these cuts have already been studied, we will not consider them any further in the present work and instead focus on separating the other three categories of event from each other.

2 Analysis Strategy and Results

2.1 Labelling Events Using the Monte Carlo Truth

We began by labelling every event using the Monte Carlo truth record in the AOD, according to which category it belonged to (see Sections 1.4 and 1.5). Duplicate copies of particles in the truth were taken into account as well as ambiguity in some steps of the chain, to ensure correct identification. The entire chain is constrained by the backbone, so it is sufficient to check that this backbone is present. Schematically, the algorithm used for each event was:

1. Iterate over all particles in the truth record until one is found that matches a possible first parent of the decay chain.
2. Iterate over the decay daughters of that particle.

[2]To be concise, we will sometimes refer to events that contain this chain exactly once with a given squark by the name of that squark (e.g. "$\tilde{t}$ events" is short for "events which contain the chain with a $\tilde{t}$ squark exactly once"). This must be understood to refer to events which contain the $\tilde{t}$ as part of our particular decay chain, not events that happen to contain a $\tilde{t}$ anywhere.

3. If the next step in the backbone is present or if the daughter is just a repetition of the parent particle, iterate over its daughters. Otherwise, conclude that the parent particle decayed by a different pathway.

4. Repeat step 3 until the bottom of the chain is reached or it is concluded the decay proceeded by a different pathway. If the bottom of the chain is reached, we conclude the chain is present.

5. If the chain is present, record every matching chain parent. Every time a match is found, compare its parent with all previous parents, to make sure it is not simply a duplicate of a previously identified chain. If it is a duplicate, ignore it, otherwise increment the number of matches found.

6. If the number of matches is exactly one, label the event according to the flavour of the parent squark, otherwise label the event as being in the category 'other'.

This algorithm was implemented in C++ using the Athena framework to access the AOD files and was thoroughly tested. Having categorised the events in this way, we can now look at reconstructed quantities for each category. This will help identify distinctive features to distinguish the events.

2.2 Missing Transverse Energy

The first quantity we considered was the missing transverse energy, $\not{E}_\perp$ because the lightest neutralino, $\tilde{\chi}_1^0$, is expected to be the LSP[10] and is also the endpoint of our decay chain (see Sections 1.1 and 1.3). Figure 3 shows histograms of $\not{E}_\perp$ for each of our four categories of event. From Figure 3 we can see that $\tilde{t}$ events have a lower missing transverse energy, on average; this may help in differentiating them.

2.3 Separating Third Generation Squarks from Other Generations

We propose b-jet tagging to differentiate the third generation $(\tilde{b}, \tilde{t})$ squarks from all the others. This is because $\tilde{b}$ and $\tilde{t}$ will decay via b and t in our chain respectively and t itself is also expected to decay overwhelmingly via b[6]. The number of b-jets in an event was defined to be the number of tagged jets with a b-tagging weight of more than 3 (see Section 1.3). Figure 4 shows histograms of this quantity for the three categories of event containing our decay chain exactly once. The third generation squark chains produce on average more b-jets, which will be useful for distinguishing them.

2.4 Separating Sbottom Chains from Stop Chains

Missing transverse energy (see Section 2.2) provides some weak discrimination potential between $\tilde{b}$ and $\tilde{t}$ chains. To better distinguish between events with $\tilde{b}$ chains and events with $\tilde{t}$ chains, we propose trying to reconstruct W bosons. One would expect events with the $\tilde{t}$ chain to contain significantly more W bosons. This is because the t quark produced will decay via a W[6] whereas a b quark will not. We tested this hypothesis by counting the number of W bosons recorded in the Monte Carlo truth information. The results are shown for $\tilde{b}$ and $\tilde{t}$ events in Figure 5. The number of W bosons per event is clearly peaked at zero for $\tilde{b}$ events and two for $\tilde{t}$ events, a significant difference.

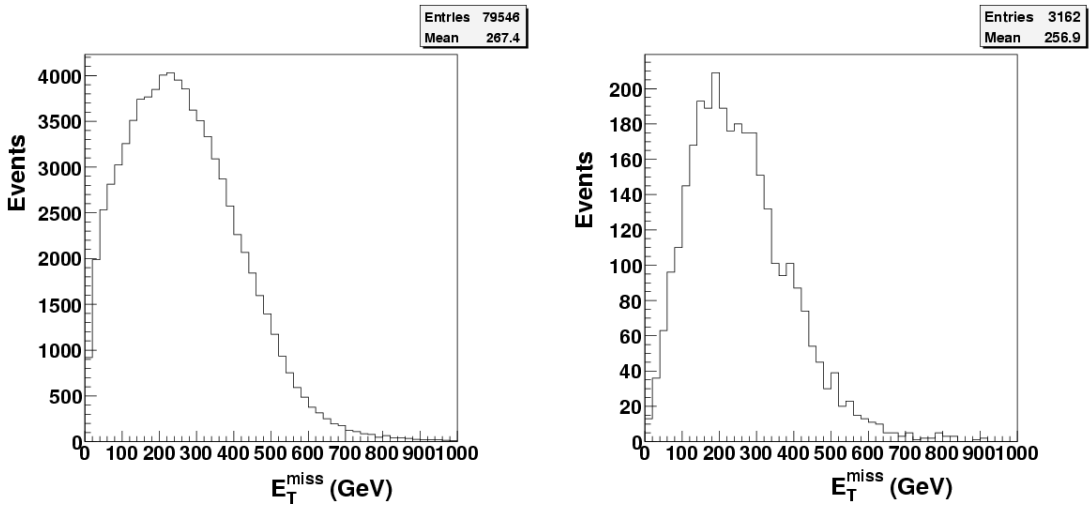

(a)

(b)

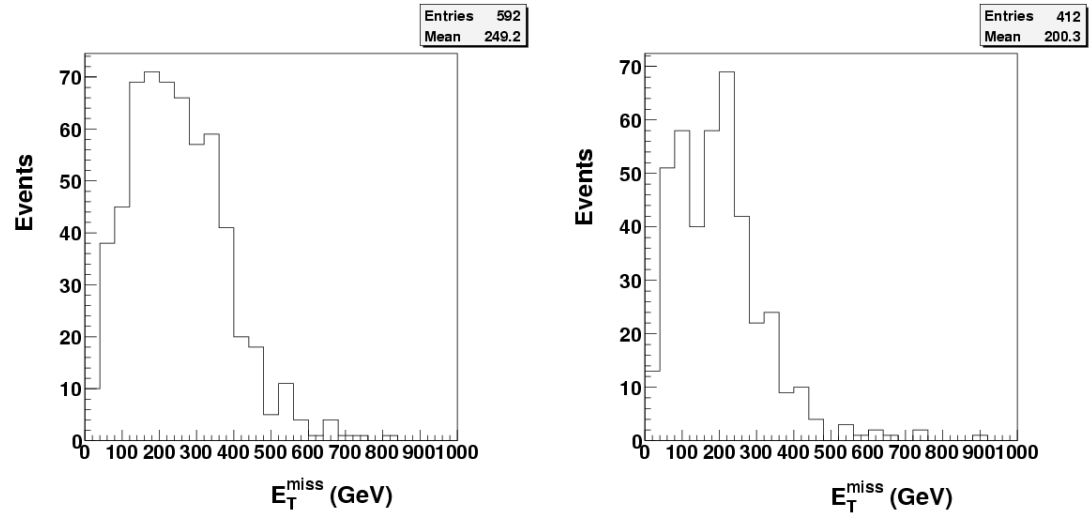

(c)

(d)

Figure 3: Histograms showing the missing transverse energy for events known to contain (a) zero, two or more of any chain, (b) either the $\tilde{d}$, $\tilde{u}$, $\tilde{s}$ or $\tilde{c}$ chain, (c) the $\tilde{b}$ chain and (d) the $\tilde{t}$ chain.

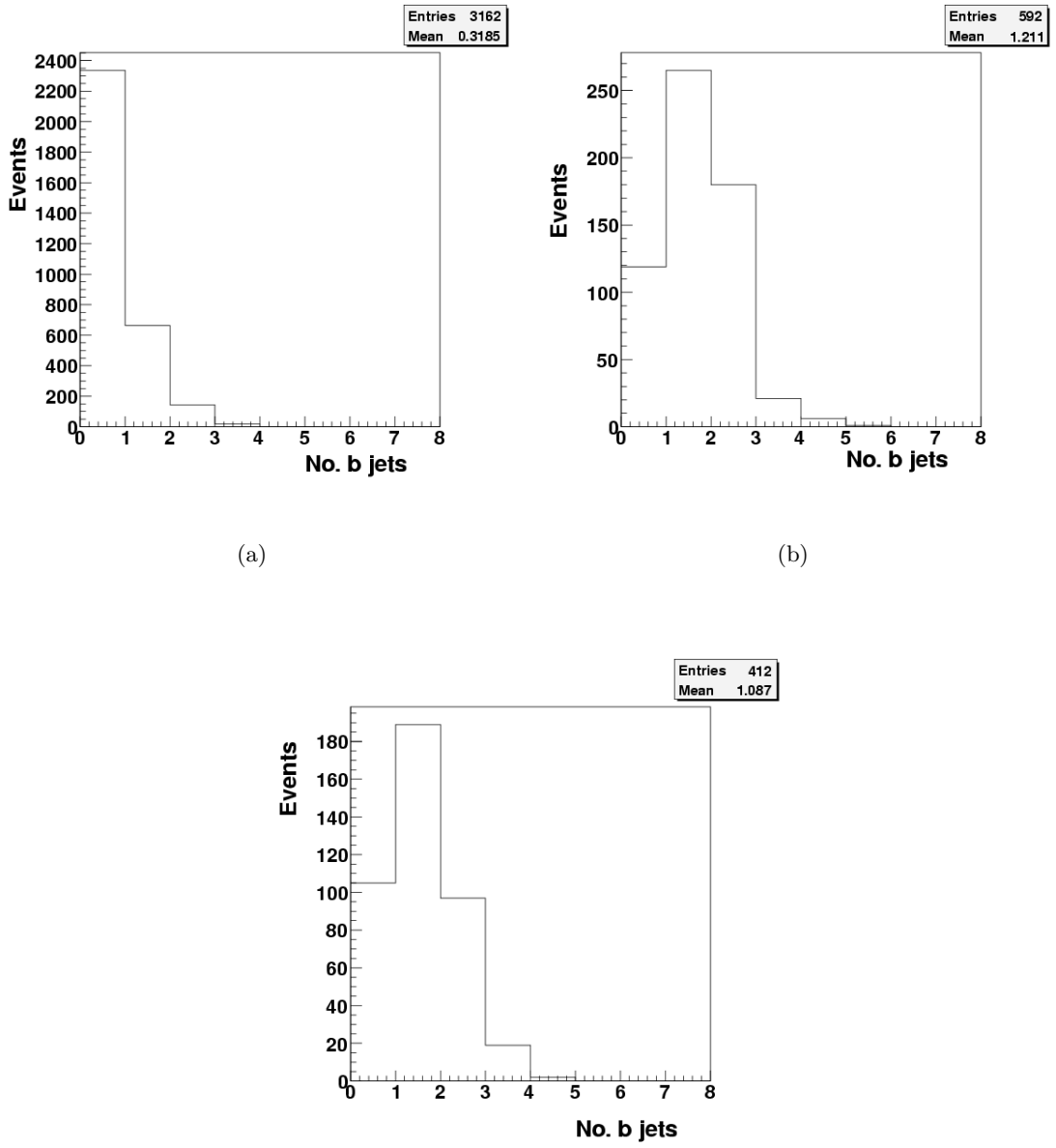

(a)

(b)

(c)

Figure 4: Histograms showing the number of b-tagged jets with with weight greater than 3 for events known to contain (a) either the $\tilde{d}$, $\tilde{u}$, $\tilde{s}$ or $\tilde{c}$ chain, (b) the $\tilde{b}$ chain and (c) the $\tilde{t}$ chain.

However, for this to be genuinely useful we must be capable of 'reconstructing' the W bosons from the detector output. This means calculating invariant mass[3] distributions and looking for peaks near the W mass, M_W. It would also be useful to reconstruct the t quark in $\tilde{t}$ events in a similar way.

2.5 Reconstructing Top Quarks and W Bosons

The t quark decays as $t \to Wb \to q\bar{q}'b$, $t \to Wb \to \bar{l}\nu_l b$ or $t \to Wb \to l\bar{\nu}_l b$. The $t \to Ws$ and $t \to Wd$ decays are highly suppressed[6].

The leptonic final states are not very useful to us – neutrinos escape the detector without being detected so it is difficult to reconstruct the W boson from this channel. However, one would expect the hadronic decay products to be detected as two jets. Fortunately, $W \to q\bar{q}'$ has a branching ratio of $\sim 68\%$[6] so we expect it to dominate, making reconstruction from jets possible in principle. We hope the b quark will also be detected and tagged as a b-jet by the detector, from which we can try and reconstruct the top mass, M_t.

For our purposes, we need to distinguish between non-b-jets (the two quarks produced in the W decay) and b-jets (produced in $t \to Wb$). Any tagged jet with weight greater than 3.0 is considered a b-jet. Non-b-jets are defined to be any jet which does not fall within a $\Delta R = 0.2$ cone of any b-jet of weight > 3.0. If a jet is within $\Delta R = 0.2$ of any b-jet with weight > 3.0 it will be used only as a b-jet. If it is within $\Delta R = 0.2$ of a tagged jet with weight < 3.0 it is used only as a jet.

We calculate two invariant mass distributions. The first, M_{jj}, is given by taking all pairs of non-b-jets and finding the invariant mass of the sum of their four-momenta. The second, M_{bjj}, is found by taking all combinations of two non-b-jets and a single b-jet. 2D plots of M_{bjj} vs. M_{jj} are given in Figure 6, for $\tilde{b}$- and $\tilde{t}$-chain events.

Figure 7 shows the M_{bjj} and M_{jj} distributions individually in 1D for the two flavours of third generation squark. From these, it can be seen that no clear peak is formed near M_W or M_t in the M_{jj} and M_{bjj} plots respectively, which we would expect to see for $\tilde{t}$ events. The attempted reconstruction has not worked.

2.6 Comparing Monte Carlo Truth with Reconstructed Quantities

To investigate the very poor reconstruction of W bosons and t quarks in $\tilde{t}$ events (see Figures 6 and 7 and Section 2.5), we returned to the truth record of the W bosons. In order to simplify the analysis, we now only consider events where we know the W decayed hadronically from the truth information. We already know that we cannot reconstruct, from jets, W bosons which decayed leptonically! We focus on trying to reconstruct the W boson because successfully reconstructing the t quark depends on this anyway.

The hadronic W truth decay products are not recorded simply as a pair of quarks. More often, there is a large number of decay products, including gluon radiation and hadrons as well as quarks. Each of these will probably not correspond to an individual jet recorded in the detector, so one cannot simply compare individual truth decay products with reconstructed jets.

To solve this, a so-called $K_\perp$ clustering algorithm[4] was run on the truth decay products. This is a longitudinally invariant method for clustering a set of four-momenta (thought to come from some common set of jets) into a desired number of '$K_\perp$ jets'. Two $K_\perp$ jets were

[3]The Lorentz invariant mass, M, is given by the relativistic formula $p^\mu p_\mu = M^2$ (in natural units), where p_μ is a four-momentum.

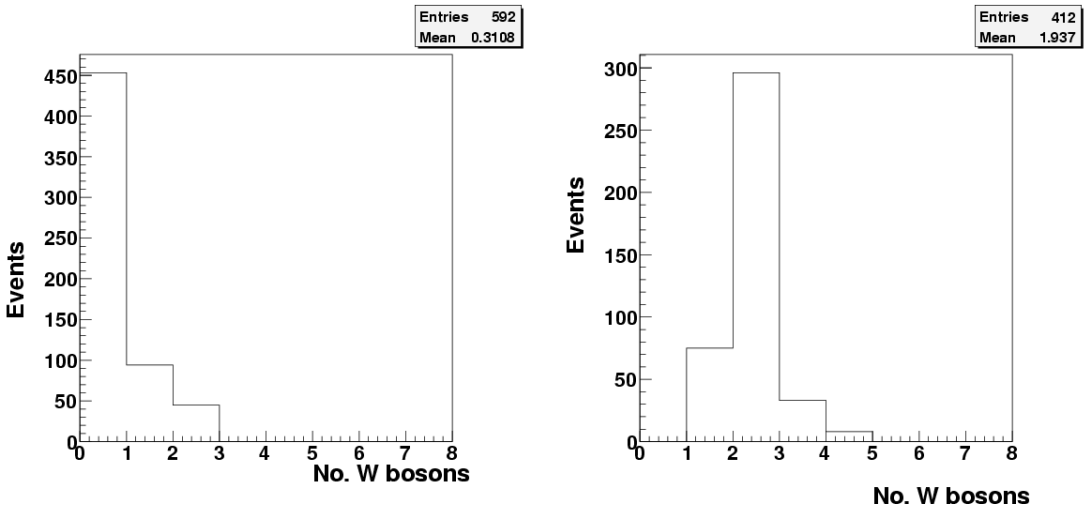

(a) (b)

Figure 5: Histograms showing the true number of W bosons for events known to contain (a) the $\tilde{b}$ chain and (b) the $\tilde{t}$ chain.

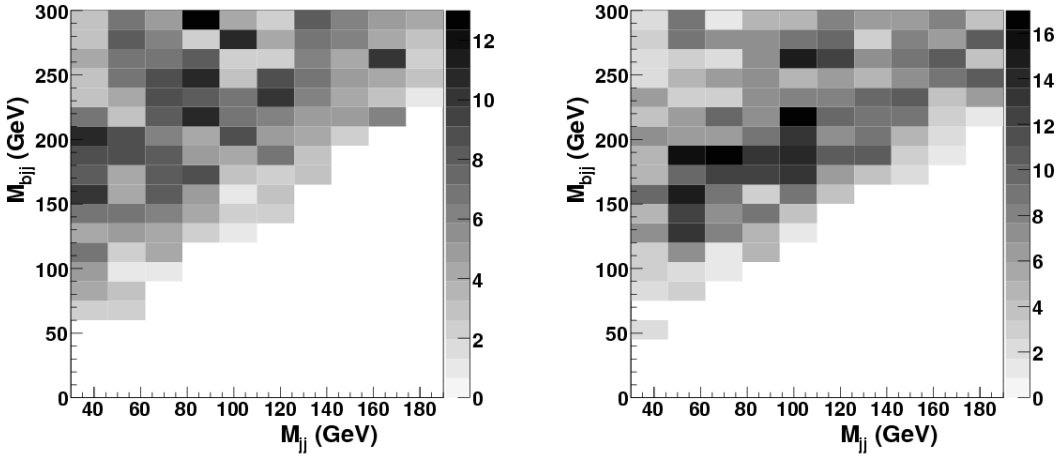

(a) (b)

Figure 6: 2D histogram showing the invariant mass distribution M_{bjj} vs. the M_{jj} distribution for events known to contain (a) the $\tilde{b}$ chain and (b) the $\tilde{t}$ chain. See Section 2.5 for details.

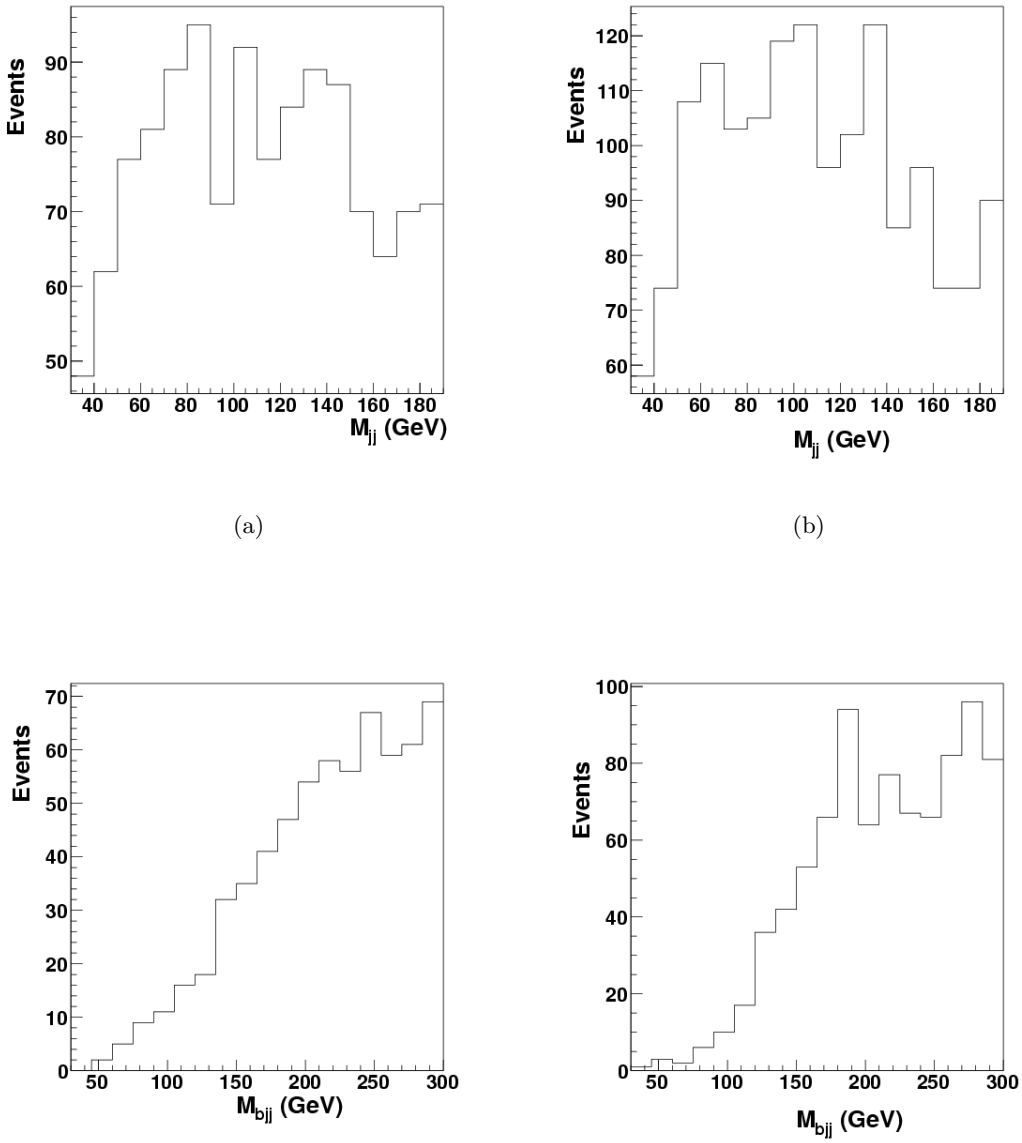

(a) (b)

(c) (d)

Figure 7: Histograms showing the M_{jj} invariant mass distribution for events known to contain (a) the $\tilde{b}$ chain, (b) the $\tilde{t}$ chain and the M_{bjj} distribution for (c) the $\tilde{b}$ chain and (d) the $\tilde{t}$ chain.

formed from our truth decay products, because we expect the W to decay into two jets. The nearest reconstructed non-b-jet in ΔR was then found for both of the $K_\perp$ truth jets. If they both matched the same jet, a second best match was found for the truth jet with lowest transverse momentum. The smallest $\Delta R = \Delta R_{min}$ was recorded. The four-momenta of the two matching reconstructed jets were added together and the invariant mass, M_{jj}, was calculated. A 2D histogram of ΔR_{min} between the truth jet and any reconstructed non-b-jet vs. M_{jj} is given in Figure 8.

As a final check, we 'cheated' and found the combination of any number of jets which yielded an invariant mass closest to M_W for each event. We then calculated ΔR between this combination and the true four-momentum of the W boson. A histogram of the number of jets in this combination vs. the invariant mass and a histogram of this ΔR are given in Figure 9.

2.7 Correlations with Missing Transverse Momentum

Because the W bosons in our decay chain did not seem to be easily reconstructed, we looked at the correlation between the $x-$ and $y-$ components of the truth W boson four-momentum, $\mathbf{w} = (w_x, w_y)$, and the missing transverse momentum (see Section 1.3), $\not{\mathbf{p}}_\perp = (p_x, p_y)$. This correlation is quantified by the cosine of the angle between them, θ, given by the two dimensional dot-product:

$$\not{\mathbf{p}}_\perp \cdot \mathbf{w} = |\not{\mathbf{p}}_\perp||\mathbf{w}| \cos\theta \Rightarrow \cos\theta = \frac{(p_x w_x + p_y w_y)}{\sqrt{(p_x^2 + p_y^2)(w_x^2 + w_y^2)}}$$

Figure 10 shows histograms of $\cos\theta$ for four different categories of truth W boson.

2.8 Differentiating Supersymmetric Decay Chains

Reconstructing W bosons and t quarks did not yield any way of distinguishing $\tilde{b}$ events from $\tilde{t}$ events. However, by using missing transverse energy (see Figure 3) and the number of b-jets present (see Figure 4), a method of distinguishing events can be devised. We will consider two quantities; the *efficiency* (number of correctly accepted events belonging to a category over the total events in that category) and the *rejection* against a particular background (the total background divided by the number of incorrectly accepted events from that background). For simplicity we will only consider discriminating between the three categories of events which contain our decay chain exactly once (see section 1.6). We propose a very simple cut-based method:

- To distinguish $\tilde{d}$, $\tilde{u}$, $\tilde{s}$ and $\tilde{c}$ from $\tilde{b}$ and $\tilde{t}$ place a cut on the number of b-jets. If an event has zero b-jets it is labelled as being $\tilde{d}$, $\tilde{u}$, $\tilde{s}$ or $\tilde{c}$Ȯtherwise it is labelled $\tilde{b}$ or $\tilde{t}$.
- If an event is labelled as $\tilde{b}$ or $\tilde{t}$, place a cut on the missing energy, $\not{E}_\perp$. Events with $\not{E}_\perp$ above a certain threshold are considered $\tilde{b}$ events, otherwise they are considered $\tilde{t}$ events.

A C++ program was written to analyse all the events and place each one in a category according to this system, as well as recording its true category. Results for distinguishing $\tilde{d}$, $\tilde{u}$, $\tilde{s}$ and $\tilde{c}$ from $\tilde{b}$ and $\tilde{t}$ using this b-jet cut are given in Table 1. The rejection quoted is against the other category. The results[4] for attempting to distinguish $\tilde{b}$ from $\tilde{t}$ events with an $\not{E}_\perp$ cut at 220 GeV are given in Table 2.

[4]Errors were estimated from the Poisson distribution – the error in a count is the square root of the number of counts – and added in quadrature.

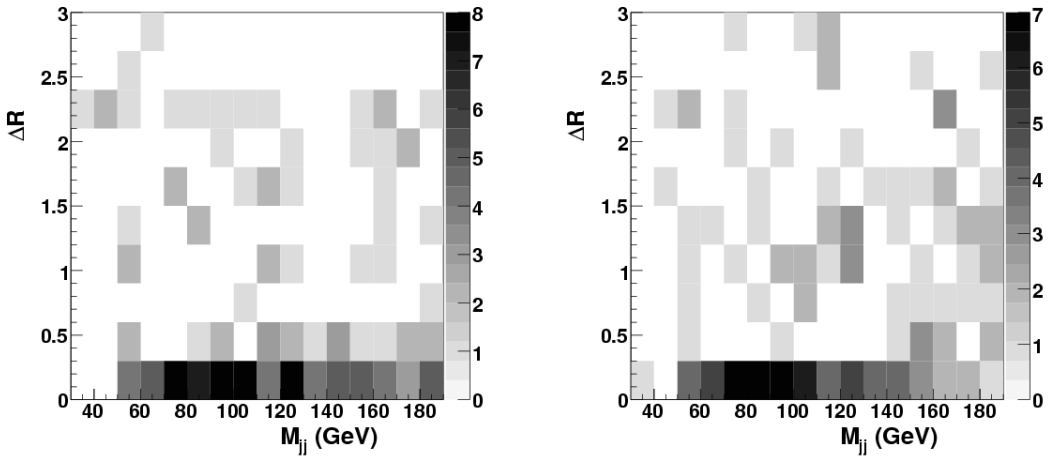

(a) (b)

Figure 8: 2D histogram showing ΔR vs. invariant mass for (a) the $K_\perp$ truth jet with highest transverse momentum ($p_\perp$) and (b) the $K_\perp$ truth jet with lowest $p_\perp$.

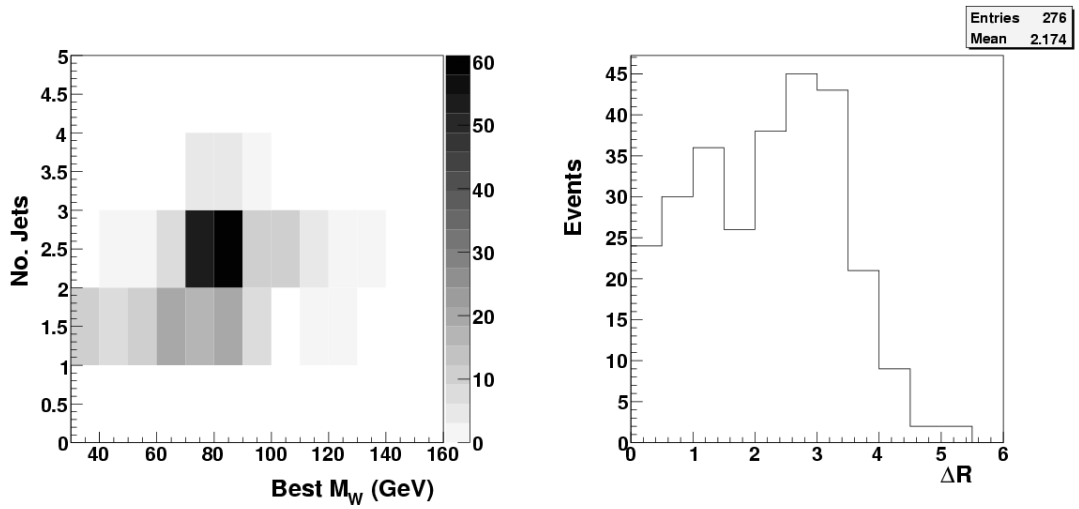

(a) (b)

Figure 9: Histogram showing (a) the number of jets which in combination yielded the closest invariant mass to M_W vs. that invariant mass and (b) ΔR between the truth W boson and that combination of jets.

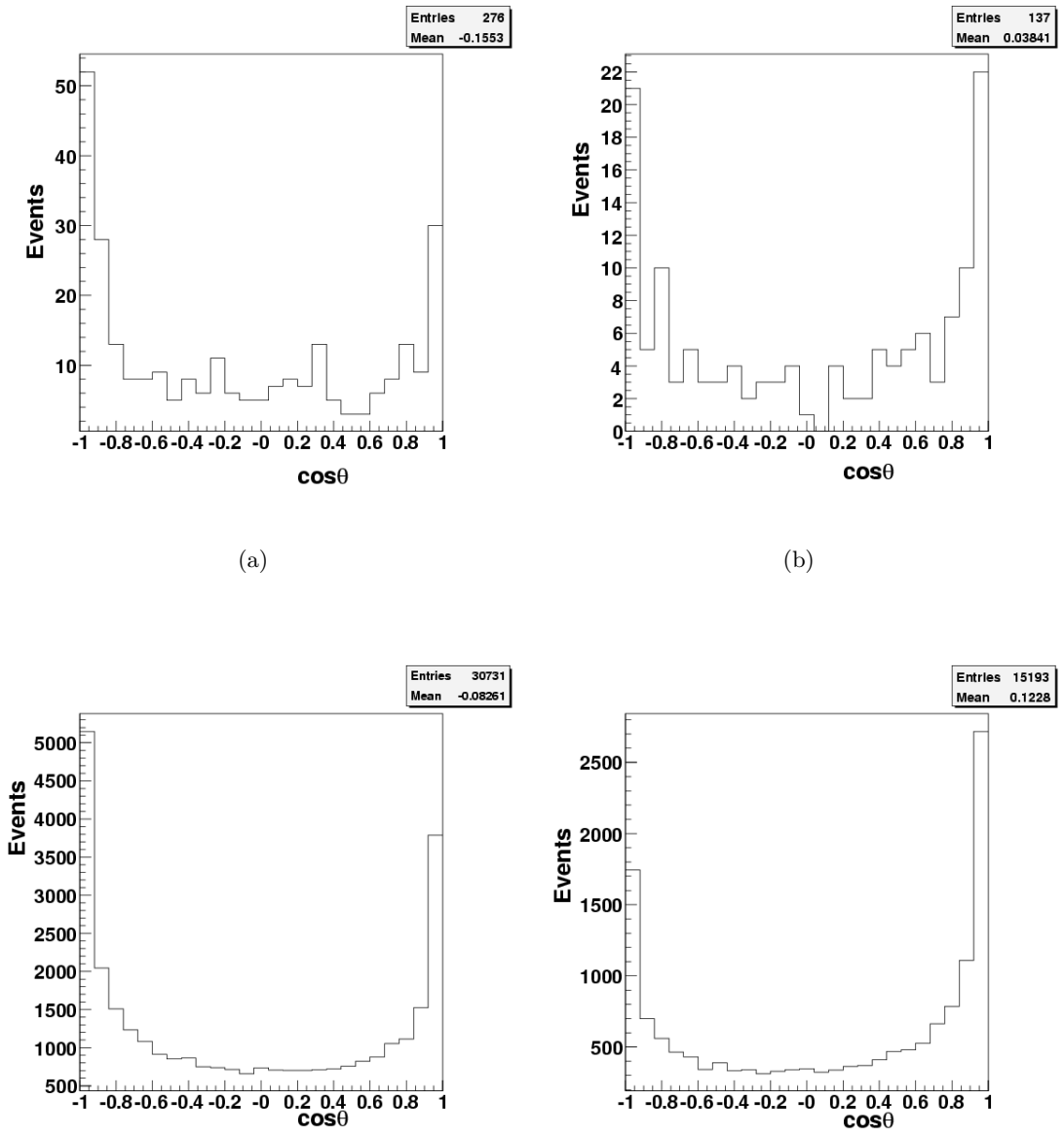

Figure 10: Histograms showing the cosine of the angle, θ, between the missing transverse momentum and truth W bosons for (a) W bosons which decay hadronically and were produced from t quarks in the $\tilde{t}$ chain, (b) W bosons which decay leptonically and were produced from t quarks in the $\tilde{t}$ chain, (c) *all* W bosons which decay hadronically and (d) all W bosons which decay leptonically.

Category	**Efficiency**	**Rejection**
$\tilde{d}$, $\tilde{u}$, $\tilde{s}$ and $\tilde{c}$	0.74 ± 0.02	4.5 ± 0.3
$\tilde{b}$ and $\tilde{t}$	0.78 ± 0.04	3.8 ± 0.2

Table 1: Table showing efficiency and rejection for distinguishing $\tilde{d}$, $\tilde{u}$, $\tilde{s}$ and $\tilde{c}$events from $\tilde{b}$and $\tilde{t}$ events using a cut on the number of b-jets.

Category	**Efficiency**	**Rejection**
$\tilde{b}$	0.44 ± 0.03	3.9 ± 0.4
$\tilde{t}$	0.49 ± 0.04	2.8 ± 0.2

Table 2: Table showing efficiency and rejection for distinguishing $\tilde{b}$ events from $\tilde{t}$ events using a missing transverse energy cut at 220 GeV.

3 Discussion

3.1 Ability to Differentiate Supersymmetric Decay Chains

Differentiating SUSY decay chains proved difficult but we still met with some success. Using a cut on the number of b-jets, it was possible to separate third generation squarks from the other two generations with high efficiency (see Table 1). However, the rejection power of this cut was relatively poor, with each category incorrectly accepting quite a high proportion of background events. We have also assumed that all events with one copy of the decay chain in any flavour are correctly identified as being so. In reality, the cuts used to separate out these events will have efficiency less than one and finite rejection, affecting the *overall* efficiency and rejection of this scheme. The number of b-jets alone is not a powerful enough cut and it would be useful to identify other reconstructed quantities to help distinguish these categories.

Distinguishing $\tilde{b}$ from $\tilde{t}$ proved even more difficult. The only quantity we found which yielded any discrimination was the missing transverse energy, $\not{E}_\perp$. However, there was still considerable overlap in $\not{E}_\perp$ between $\tilde{b}$ and $\tilde{t}$. The results of cutting at 220 GeV are shown in Table 2. Both the efficiency and rejection of this cut are very poor – a very high proportion of events are misidentified. Furthermore, each sample is also contaminated with $\tilde{d}$, $\tilde{u}$, $\tilde{s}$ and $\tilde{c}$ events because of the low rejection of the b-jet cut mentioned above.

One could improve the efficiency with which $\tilde{t}$ events are identified and rejected from $\tilde{b}$ by raising the $\not{E}_\perp$ cut. However, this entails a concomitant loss in the efficiency of identifying $\tilde{b}$ events and their rejection from $\tilde{t}$. $\not{E}_\perp$ is a poor quantity with which to differentiate the third generation squarks from each other and there is a need to discover better ways. Worse still, it is unclear why $\tilde{t}$ events should have the lowest $\not{E}_\perp$ on average. This may be dependent on which point in mSUGRA parameter space we are considering and would require further work to explain. Hence, this method may not generalise very well.

We tried to distinguish between events using hard-cuts, i.e. by asking yes-or-no questions. One could imagine a system which instead gives every event a weighting. This weighting would be calculated by how close some property of an individual event is to some threshold. If several quantities were available for consideration, such weightings could be combined, to

yield an overall value for each event. By comparing this value to some ultimate yes-or-no cut, events could be categorised. Anyway, the effectiveness of the weighting could be gauged by making histograms of it for each category of event. However, it would require many free parameters, which would have to be experimentally determined. This is an area for further research, as well as finding other quantities which provide better discrimination.

3.2 Difficulties Reconstructing W Bosons and Top Quarks

The difficulties in distinguishing $\tilde{b}$ events from $\tilde{t}$ events stem from our failure to find a reconstructed quantity which provides strong discrimination. According to the Monte Carlo truth record though, the number of W bosons per event should provide just that (see Figure 5). The presence of t quarks in the $\tilde{t}$ events should also yield help.

However, the M_{bjj} vs. M_{jj} plots (see Section 2.5 and Figure 6) show only a slight excess of events around the point $M_W \simeq 80.4$ GeV, $M_t \simeq 174$ GeV for $\tilde{t}$-chain events compared to $\tilde{b}$. There is no convincing sign of a peak at M_W in the $\tilde{t}$ 1D M_{jj} distribution even though we know those events contained W bosons (see Figure 5(b)). Neither is there a clear signal at M_t in the M_{bjj} distribution for $\tilde{t}$ events. These distributions are of no use in distinguishing $\tilde{b}$ events from $\tilde{t}$ events.

To calculate these invariant mass distributions, jets had to be labelled as either non-b-jets or b-jets, because of the decay mode we were attempting to reconstruct (see section 2.5). The method of assignment depends on two free parameters. The parameters used (requiring a $\Delta R < 0.2$ match to a b-jet with weight > 3) were certainly sensible, but it is not known what effect varying them would have on the success of the reconstruction. It is also inconvenient that the b-jet tagging container in the AOD is different to the plain jet container (see Section 1.4) so one can't directly see if a jet is likely to be a b-jet.

3.3 Difficulties Comparing Monte Carlo Truth to Reconstructed Quantities

The comparison between truth particles and reconstructed quantities was difficult because of the hadronisation of the truth W decay daughters. We tried to overcome this by using a $K_\perp$ clustering algorithm, to form just two jets from all the daughters and comparing these to reconstructed jets. It can be seen from Figure 8 that while the $K_\perp$ truth jets often have a relatively good ΔR match to a reconstructed non-b-jet, these matching jets still do not reconstruct very closely to $M_W \simeq 80.4$ GeV at all.

We also found the combination of any number of jets which yielded an invariant mass closest to M_W and compared it to the truth W boson four-momentum in ΔR. This is not a valid reconstruction strategy in general and could not be used to help distinguish between our categories of event because it is self-fulfilling.

From Figure 9, we can see that this combination is usually made of two jets, it is nowhere near the truth W because the ΔR distribution has a mean[5] of 2.17 ± 0.09. Even if this 'single best guess' didn't actually correspond to our W boson every time, one would expect it to match more often (if the W decay products were being detected) than is seen. This would result in more events with low ΔR.

[5]The error was estimated using the central limit theorem

3.4 Relation to the Missing Transverse Energy

The evidence above suggests that the hadronic decay products of the W boson produced in our decay chain are not always being detected, so we looked at the correlation between the missing transverse momentum and the truth W boson. This is given in Figure 10, which is a histogram of the cosine of the angle between these two-vectors in the transverse plane (see Section 2.7).

Remembering that $\cos 0 = 1$ and $\cos \pi = -1$, Figure 10 shows interesting correlations and anti-correlations between the missing transverse momentum, $\not{\mathbf{p}}_\perp$, and transverse momentum of truth W bosons, $\mathbf{w}$. If our inability to detect the W bosons was solely caused by an elementary bug in the C++ analysis code, it would seem likely this distribution would be uniform (no correlation at all). This gives at least some assurance this is not the case.

When $\not{\mathbf{p}}_\perp$ is anti-correlated with $\mathbf{w}$ we infer that the decay products were detected (see Section 1.3). This happens $(34 \pm 4)\%$ of the time. However, $(19 \pm 3)\%$ of the time, $\mathbf{w}$ is *correlated* with the missing energy, when the W from our chain decayed hadronically. As we expected, this correlation is observed a greater proportion of the time when the W decays leptonically, $(29 \pm 5)\%$. This same pattern is seen when considering *every* truth W boson in every event. $(20.0 \pm 0.5)\%$ of the time we see a strong correlation with the missing energy for W bosons which decay hadronically. When they decay leptonically, this happens $(31 \pm 1)\%$ of the time.

The correlation with $\not{\mathbf{p}}_\perp$ suggests that the decay products of our W boson escaped without being detected, at least some of the time. Furthermore, all W bosons seem to have a similar correlation with $\not{\mathbf{p}}_\perp$, which implies they would also be hard to reconstruct.

This apparent $\sim 20\%$ rate of W boson disappearance, combined with the $\sim 68\%$ branching ratio to the hadronic decay may explain the poor reconstruction. These factors would mean that in $\sim 46\%$ of $\tilde{t}$ events, our attempted reconstruction would definitely fail. Any signal would be obscured by all the events where there simply aren't any jets that reconstruct to our W boson. This agrees with the poor invariant mass distribution seen in Figure 7.

3.5 Possible Improvements and Further Work

Further work is needed to investigate the reasons behind the poor reconstruction and how significant the effect is. One cannot rule out that there is a bug in the code responsible for producing the simulated detector output, though this seems unlikely. Trying to determine if such a bug exists and searching for it would be a massive undertaking. It is also possible that the particles escape through cracks in the detector, where different components join up. To investigate this theory would also represent substantial further work.

By naïvely combining every pair of non-b-jets, a clear signal did not emerge at M_W. It may be possible to overcome the deleterious effects discussed above using a more sophisticated reconstruction method, e.g. by excluding some of the jets in the event or only selecting combinations which fulfill some criteria. Such a strategy risks being arbitrary and self-fulfilling and would require careful consideration of the physics motivation to avoid this. It would also require an investigation into how useful it would be for discrimination.

A possible improvement is to see which $\tilde{t}$ events fail the cuts that were proposed for separating out events with zero, two or more of any flavour of chain (see Section 1.6). Their removal could result in a clearer signal from the remaining events because the cuts require four or more high transverse momentum jets, potentially ruling out events where the W boson decay products 'disappeared'. This too would require further investigation.

4 Conclusions

In conclusion, we achieved modest discrimination between events containing the $\tilde{d}$, $\tilde{u}$, $\tilde{s}$ or $\tilde{c}$ and events with either the $\tilde{b}$ or $\tilde{t}$ chain by using a cut on the number of b-jets (see Table 1). Very poor differentiation was achieved between $\tilde{b}$ and $\tilde{t}$ events using a missing transverse energy cut (see Table 2). It had been hoped we could reconstruct W bosons and t quarks in our $\tilde{t}$ events to tell them apart form $\tilde{b}$ events, but this has not proved possible. Searching for other reconstructed quantities and methods to see if better discrimination is possible is an opportunity for further work. The ability to separate these decay chains by flavour has important consequences for future SUSY studies and reconstructing the SUSY mass spectrum.

We investigated why it was so hard to reconstruct the W bosons in our events. It was found that in least $\sim 20\%$ of hadronic W decays, their decay products were seemingly not being detected. We cannot draw any definite conclusions as to why this is or how significant it is, and this represents another area for further research.

5 Acknowledgements

I would like to thank Chris Lester, Martin White, Luca Fiorini, James Frost and everyone at the Cambridge Supersymmetry Working Group for their help and support, without which this project would not have been possible.

Appendix A: Efficient Analysis of Full Simulation Data

Athena takes $\sim$ 2 hours to run over the $\sim 80,000$ events ($\sim$ 8 GB of data) used in this analysis. Besides this, compiling Athena programs involves linking against a massive code library and using cumbersome code management software, which is also slow. To speed up the development and analysis time, we wrote Athena code to save the quantities we were interested in as a plain text file and ran this once. A standalone C++ program was then written to parse this file and carry out analysis on the events. In this way, we could run over all the events in $\sim$ 1 minute. This is a useful method for speeding up the analysis of full-simulation data. The drawback is that it is slightly restrictive – if there is some quantity in the AOD not saved as plain text, one must return to Athena and recreate the file. Still, it is vastly more efficient than using Athena on its own.

Sadly, this step was not taken until some way into the present work, so the gains could have been greater. Even though it represents a massive increase in efficiency, writing this software took time away from the physics analysis. This is why we somewhat delayed developing it.

Appendix B: Correction to Histograms

Unfortunately, *every histogram in this report* contains a single duplicate entry. This was due to a bug in the software we wrote to draw the histograms and was discovered too late to correct. However, this is almost completely negligible and does not seriously affect the present analysis.

References

[1] List of SUSY samples for Rome.
https://uimon.cern.ch/twiki/bin/view/Atlas/RomeSUSYWiki.

[2] *ATLAS Detector and Physics Peformance TDR.* CERN, 1999.

[3] B. C. Allanach, C. G. Lester, M. A. Parker, and B. R. Webber. Measuring sparticle masses in non-universal string inspired models at the LHC. *JHEP*, 0009:004, 2000.

[4] S. Catani, Y. L. Dokshitzer, M. H. Seymour, and B. R. Webber. Longitudinally-invariant $k_\perp$-clustering algorithms for hadron-hadron collisions. *Nuclear Physics B*, 406:187–224, September 1993.

[5] D. Cavalli and S. Resconi. Comparison between full simulation and fast simulation of ATLAS detector. 1997. ATLAS internal note.

[6] S. Eidelman et al. Review of Particle Physics. *Physics Letters B*, 592:1+, 2004.

[7] I. Hinchliffe and G. Stavropoulos. Atlas Monte Carlo Interfaces.
http://www-theory.lbl.gov/∼ianh/monte/Generators/.

[8] S. Kotov. b-tagging in ATLAS. 2005. Slides for Max Planck Institute für Physik seminar.

[9] S. Lloyd et al. The ATLAS Workbook.
https://twiki.cern.ch/twiki/bin/view/Atlas/WorkBook.

[10] S. P. Martin. A Supersymmetry Primer, 1997.

[11] E. Richter-Was, D. Froidevaux, and L. Poggioli. ATLFAST 2.0: A fast Simulation package for ATLAS. 1998. ATLAS internal note.